Numerical simulations for isostatic and die compaction of powder by the discrete element method

J.-F. Jerier[1], B. Harthong[1], V. Richefeu[1], D. Imbault[1], F.-V. Donzé[1,1], P. Dorémus[1]

[a] *University of Grenoble, L3S-R UMR5521 UJF/INP/CNRS, Domaine universitaire, BP 53, 38041 Grenoble Cedex 9, France.*
[b] *QCAT,CSIRO, PO Box 883, Kenmore, QLD, 4069, Australia.*

Abstract

The Discrete Element Method, based on a soft-sphere approach, is commonly used to simulate powder compaction. With these simulations a new macroscopic constitutive relation can be formulated. It is able to describe accurately the constitutive material of powders during the cold compaction process. However, the force law used in the classical DEM formulation does not reproduce correctly the stress evolution during the high density compaction of powder. To overcome this limitation at a relative density of about 0.85, the high density model is used. This contact model can reproduce incompressibility effects in granular media by implementing the local solid fraction into the DEM software, using Voronoi cells. The first DEM simulations using the open-source YADE software show a fairly good agreement with the Multi-Particle Finite Element (MPFEM) simulations and experimental results.

Key words: Powder compaction, Discrete element method, Multi particle finite element method

1. Introduction

Powder metallurgy has long been an attractive process technology for both advanced and conventional materials. In a forming operation, powder is consolidated into a desired shape, normally by applying pressure. After forming, the green body (i.e., the compacted body) is sintered so that the mechanical resistance of the final component is effective [2]. Using powder

compaction can save both time and money in the manufacture of mechanical parts in serial production. One of the major advantages is that near net shape parts produced by this method need little or no machining. Another significant advantage is the possibility to design the material properties by mixing different powder materials so that the final product achieves a specifically desired mechanical behavior. This results in a very high density (i.e., compact density greater than 0.9) conducive to forming a more homogeneous material suitable for high strength applications.

But in the powder compaction process, plasticity and elasticity phenomena, internal friction of porous medium and frictional effects between the die walls may induce inhomogeneous distributions of density and residual stress [3]. As a consequence, cracks appear into the compacted zone during the pressing process and the mechanical behavior of that part is difficult to predict [16]. To understand the complicated behavior of the powders, industrials have performed expensive trial and error procedures. With this in mind, numerical methods can be considered as a cheap and easy solution to help the prediction of the product properties, but the two numerical approaches known based on the finite element method (FEM) [21, 15] and the discrete element method (DEM) [7, 8] reproduce these phenomena with some difficulties. These obstacles are mainly due to the nonlinear material behavior during the pressing step [6].

Nevertheless, understanding and predicting the mechanical behavior of the final component can be done by the micro-mechanic simulation with adequate phenomenological models. These models may mimic the compaction process [9], because the DEM can give interesting insight on the different physical phenomena present during the early stage of powder compaction [16, 22].

In this paper, we use a new micro-mechanic model to perform discrete numerical simulations of powder compaction up to a density equal to 0.95. In section 2, we present the existing and new discrete models which are developed to simulate the powder process. Then in section 3, the simulations of isostatic and die compaction of random packings are performed with both the existing and the new discrete models. The results are then compared to experimental results or the multi-particle finite element method (MPFEM) simulations [17, 4].

2. Discrete models

In DEM, the motion of each particle is resolved by using an explicit integration method from Newton's second law [20]. The force and moment that act on each particle result from the interaction forces with their neighboring particles and these forces are numerically computed by means of a *force-law* (i.e. an explicit relation between the force components and the local parameters). The DEM can easily simulate complex constitutive mechanical behaviors of granular materials with force-laws which integrate physical parameters, due to the discrete character of the sample. In this section, we present the force-laws commonly used to model the powder compaction and we introduce a new contact model (so called high density model) developed to simulate the compaction up to a high density value. Only material parameters are required for these models and no calibration is needed.

2.1. Existing models

In the simulations of compaction based on DEM, the powder is often represented by elastic-plastic spheres. The elastic part of the contact force is generally given by the Hertz contact law that expresses the normal elastic force F_{ij}^e between two spheres i and j as a function of their overlap h_{ij}. This force-law reads:

$$F_{ij}^e = \frac{4}{3}\left(\frac{1-\nu_i^2}{E_i} + \frac{1-\nu_j^2}{E_j}\right)^{-1} \sqrt{R_{ij}^\star}\, h_{ij}^{3/2}, \tag{1}$$

where $R_{ij}^\star = (R_i R_j)/(R_i + R_j)$ is the reduced radius of the particle i and j, E_i and E_j are the Young's moduli of their constitutive materials, and ν_i and ν_j are their Poisson coefficients.

During compaction, particles in contact deform irreversibly and thus the plastic deformation of the constitutive material of the particles must be taken into account. The plastic force-law of Storåkers is generally used for this purpose. In the limiting case of a rate-independent material, it is based on a rigid-plastic Von Mises-type material with strain-hardening defined as:

$$\sigma = \sigma_0\, \varepsilon^{\frac{1}{m}}, \tag{2}$$

where σ and ε are respectively the uniaxial Von Mises equivalent stress and strain, σ_0 and m are material constants. The force-law derived by Storåkers

[19] gives the normal plastic force F_{ij}^p between the particles i and j as a function of the plastic parameters σ_0 and m of the particles:

$$F_{ij}^p = \pi\sigma_0 \; 2^{\frac{2m-3}{2m}} 3^{\frac{m-1}{m}} \{c(m)\}^{\frac{2m+1}{m}} (R_{ij}^\star)^{\frac{2m-1}{2m}} (h_{ij})^{\frac{2m+1}{2m}}, \tag{3}$$

where $c(m) = \sqrt{1.43e^{-0.97/m}}$ is related to the area of the contact zone. This plastic force-law has been derived from finite element analyses and Hill's theory on the indentation of a rigid sphere with a deformable plane [11].

Some authors have used Storåkers's model (see Eq. 3) coupled with the Hertz contact (see Eq. 1) to perform discrete element simulations of powder compaction [5]. Nevertheless, this approach is limited in density, because it assumes the mechanical and geometrical independence of the contacts. Hence particles are considered to have only local deformation in the contact zones applied. These are small compared to the particles' sizes, and far from each other, such that there is no influence of the neighboring contacts. In theory, this assumption limits the model validity to the cases where interferences between the contacts are negligible [18], but it is generally accepted that the model is valid up to a relative density (i.e. the ratio of the volumetric mass of the powder relative to the volumetric mass of the material of its particles) of about 0.85. The model presented in the following overcomes this limitation by taking into account the contact interferences by means of a definition of the local solid fraction.

2.2. high density model

The high-density compaction analysis must absolutely account for the influence on each contact force of all the contacts around the particles. In the proposed model, this influence of these neighboring contacts are considered in an indirect way by using the concept of Voronoi cell as suggested by Arzt [1]. When a weighted 3D Voronoi partition of the packing is performed, the sum of all cell volumes correspond to the packing volume and each powder particle (initially spherical) are surrounded by a Voronoi cell that contains its own solid fraction (see Fig. 1). It is thus easy to define from the weighted Voronoi partition, a *local solid fraction* associated with a particle i:

$$\rho_i = \frac{4}{3}\frac{\pi R_i^3}{V_i}, \tag{4}$$

where V_i is the volume of the Voronoi cell surrounding the particle i. It is interesting to note here that $\rho_i = 1$ means that the volume of the cell is completely filled by the material originally contained in the particle i.

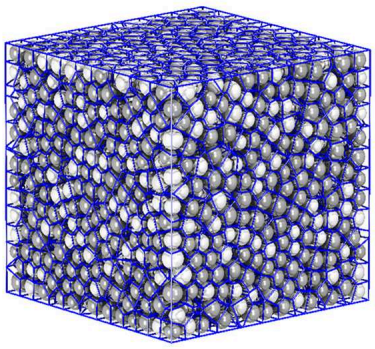

Figure 1: Packing of 4000 spheres represented with the associated Voronoi cells.

To derive a force-law for the discrete element simulation of high density compaction, Harthong et al. [10] introduced a solid fraction ρ_{ij} defined at the contact level between particles i and j. In our implementation and in a first approximation, we arbitrarily defined this parameter as the average solid fraction of the adjacent cells i and j:

$$\rho_{ij} = \frac{1}{2}(\rho_i + \rho_j). \tag{5}$$

From finite element simulations of isostatic compaction of a cubic unit cell containing one spherical particle (Fig. 2), Harthong et al. attempt to identify a force-law able to reflect the elastoplastic flow of the particles. The initial solid fraction of the unit cell was $\rho^0 \simeq 0.52$. The high density force-law gives the normal force F_{ij} between the particles i and j as a function of the parameters σ_0 and m of the particles. It has been formulated in the case where both spheres are identical, with the same radius R :

$$F_{ij}(t + \Delta t) = F_{ij}(t) + 2\sigma_0 R S_{ij}(m, \frac{h_{ij}}{R}, \rho_{ij})\, \Delta h_{ij}(t) \tag{6}$$

In this relation, the stiffness S_{ij} depends both on material and geometric parameters:

$$S_{ij} = \alpha_1(m)\mathrm{e}^{\beta_1(m)\frac{hij}{R}} + \alpha_2(m)\mathrm{e}^{-\beta_2\frac{h_{ij}}{R}} + \alpha_3(m)\frac{[max(0, \rho_{ij} - \rho^0)]^2}{1 - \rho_{ij}} \tag{7}$$

where ρ^0 is the reference solid fraction resulting from the identification procedure of the law, and $\alpha_1, \alpha_2, \alpha_3, \beta_1$ and β_2 are parameters that depend only

on m:

$$\begin{cases} \alpha_1(m) = 0.97 - 0.58/m \\ \alpha_2(m) = \frac{15}{1+3/m} - 4 \\ \alpha_3(m) = 15\,(1 - 1/2m) \\ \beta_1(m) = 1.75\,(1 + 1/2m) \\ \beta_2 = 8 \end{cases} \tag{8}$$

In the present work, it is assumed that this *force-law* can be extended to small polydispersity by replacing R by $2R^{\star}_{ij}$.

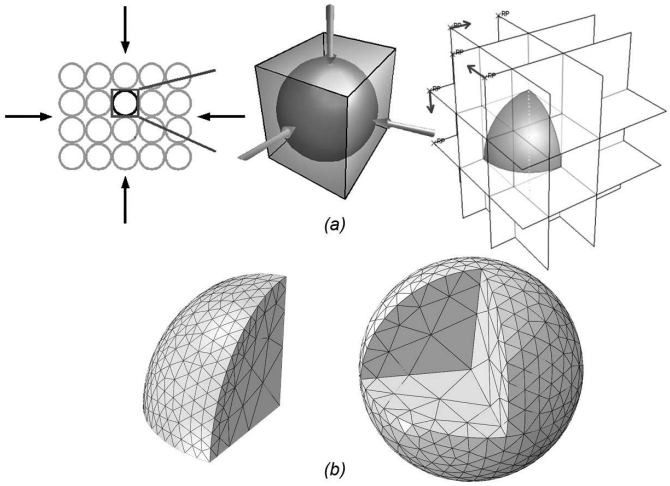

Figure 2: The compaction of an ordered packing with the multi-particle finite element method used to develop a new normal force-displacement law for DEM simulations.

In the next section, we use the high density force-law to simulate isostatic and die compaction of a sphere packing. The stress–relative density curves are then compared with the results obtained with Storåkers' model and the multi-particles finite element method (MPFEM) used to develop the high density force-law.

3. Simulations and results

To assess the validity of the high density force-law, we performed simulations of isostatic and die compaction with both DEM and MPFEM (Fig. 3). We used the same initial packing of 32 spheres of radius $R = 0.15$mm placed inside a cube of 1 mm side. The spheres are made of lead ($\sigma_0 = 20.5$ MPa and $m = 4.17$) and we also picked the copper parameters ($\sigma_0 = 500$ MPa and $m = 3.33$) to allow comparison with experimental data from literature [5]. The number of spheres was limited to keep a reasonable calculation time for the MPFEM implemented in the software ABAQUS. The DEM simulations were performed using the open-source code YADE [14] where the models described in Section 2 were implemented.

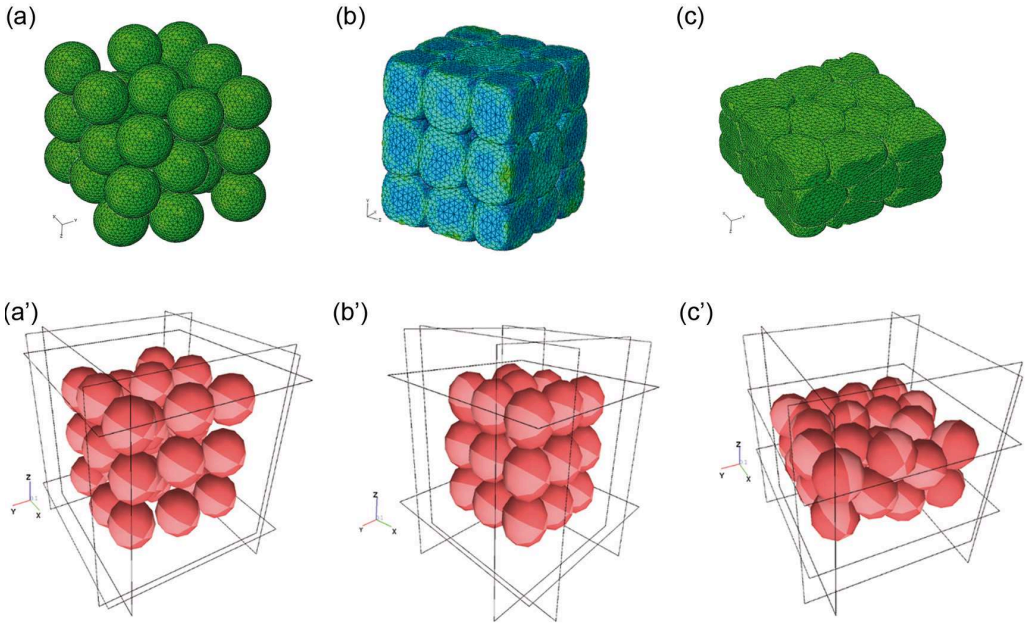

Figure 3: The same assembly of 32 monosize spheres used for the MPFEM and DEM simulations. (a-b-c) 32 meshed spheres and compacted with the MPFEM for isostatic (b) and die (c) loading. (a'-b'-c') 32 spheres compacted with the DEM for isostatic (b') and die (c') loading on YADE software

3.1. Isostatic compaction

In the case of isostatic compaction, all six box walls moved inward at a constant velocity. During the simulations, the relative density of the packing

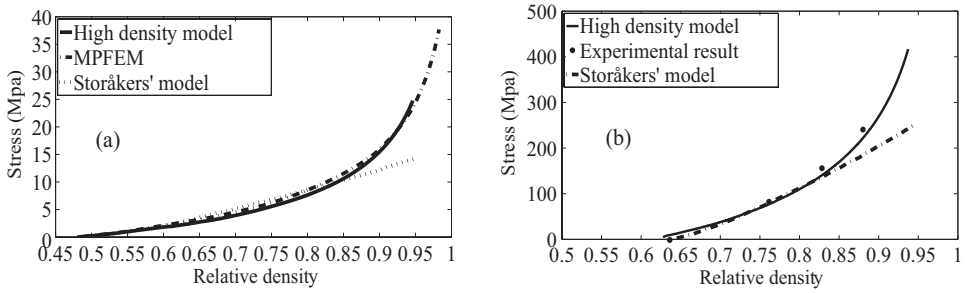

Figure 4: (a) Comparison between the new contact law, the MPFEM and the Storakers's law for isostatic compaction of 32 spheres made of lead ($K' = 20.5$ MPa, $n = 0.24$) in a random packing, without friction. (b) Comparison for an isostatic compaction of powder copper ($K' = 500$ MPa, $n = 0.3$) between an experimental result done by James in 1997, Storåkers' law and the new analytical contact law.

was measured together with the pressure on each wall and we checked that all six measured stresses were equal with a good precision. Figure 4(a) shows the stress–density curves obtained by using the MPFEM and the DEM with the force-laws presented above. The results obtained by the MPFEM close to the experimental results [4] and they represent the reference results for our validation.We observe a nice agreement between the MPFEM ans DEM results with the high density model up to a relative density value equal to 0.95. On the other hand, Storåkers' model clearly gives a wrong response for relative densities greater than about 0.85. It is important to note here that no calibration was necessary in our simulations and the only parameters used can be fairly easily obtained from experimental tests on the particle's material. We illustrate this through Fig. 4(b) that shows a comparison between the high density model of Harthong et al., experimental data from James (1997) [5][12] and Storåkers' model, in the case of an isostatic compaction of copper. We used for these simulations a packing of 4000 spheres generated by a geometric algorithm [13] (see Fig. 1).

3.2. Die compaction

In the case of die compaction, the sample of frictionless 32 spheres is compacted along the Z-axis by moving the horizontal walls towards one another at a constant velocity, whereas the vertical walls are kept fixed (see Fig. 3). The stress-density curves resulting from the simulation of die compaction

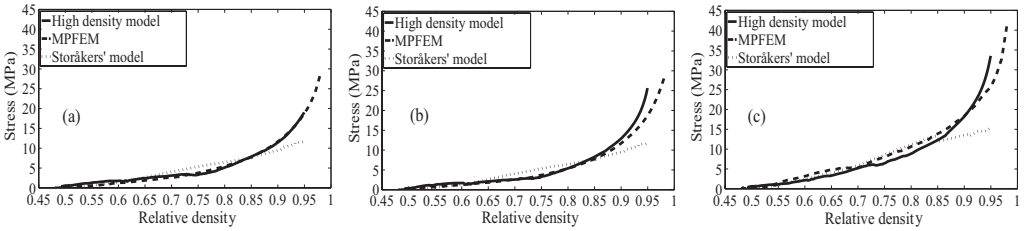

Figure 5: Comparison DEM curves computed with YADE and MPFEM curve computed with ABAQUS for die compaction of 32 spheres of lead in random packing, without friction.

of lead spheres are shown in Fig. 5 for the three space directions. We still observe a good agreement of our simulation curves with the reference curves obtained with MPFEM whatever the relative density lower than 1. A limit at a relative density of about 0.85 is observed when using Storåkers' model for die compaction.

4. Concluding remarks

In the DEM, the study of the force-law in a random packing of spheres submitted to high density compaction is essential for numerical simulation. The MPFEM method used is based on precise and quantifiable data. But for the moment, it still requires an unaffordably long calculation time compared to the discrete element method. With the introduction of a new parameter which represents the local solid fraction, the effects of plastic incompressibility into the sphere packing can be modeled in the DEM framework, allowing the description of high-density effects. The results presented above are encouraging, and show that the high density model proposed here can potentially lead to an interesting accuracy. Indeed, this approach showed that it is possible to completely reproduce experimental result for isostatic compaction. To perform DEM simulations of industrial powder with irregular shape particles, this approach will be kept and the model will also need to account for the cohesion and the friction law at the contact.

References

[1] E. Artz. Influence of an increasing particle coordination on the densification of spherical powders. *Acta Materiall*, 30:1883–1890, 1982.

[2] D. Bouvard. *Metallurgie des poudres*. Hermes Science, 2002.

[3] P.R. Brewin, O. Coube, P. Doremus, and J.H. Tweed. *Modelling of Powder Die Compaction*. Engineering Materials and Processes, 2008.

[4] Y. Chen, D. Imbault, and P. Dorémus. Numerical simulation of cold compaction of 3d granular packings. *Materials Science Forum*, 534-536:301–304, 2006.

[5] C.L. Martin C.L., D. Bouvard, and S. Shima. Study of particle rearrangement during powder compaction by the dem. *Journal of the Mechanics and Physics of Solids*, 51:667–693, 2003.

[6] A.C.F. Cocks. Constitutive modelling of powder compaction and sintering. *Progress in Materials Science*, 46:201–229, 2001.

[7] P.A. Cundall and O.D.L. Strack. A discrete numerical model for granular assemblies. *Geotechnique*, 29:47–65, 1979.

[8] F.V. Donzé, V. Richefeu, and S.-A. Magnier. State of the art of geotechnical engineering, electronic journal of geotechnical engineering. *Advances in Discrete Element Method applied to Soil, Rock and Concrete Mechanics*, pages 1–44, 2009.

[9] N.A. Fleck. On the cold compaction of powder. *Journal of the Mechanics and Physics of Solids*, 43:1409–1431, 1995.

[10] B. Harthong, J.-F. Jerier, P. Dorémus, D. Imbault, and F.-V. Donzé. Modelling of high-density compaction of granular materials by the discrete element method. *International Journal of Solids and Structures*, submitted, 2009.

[11] R. Hill, B. Storakers, and A.B. Zdunek. A theoretical study of the brinell hardness test. *Royal Society of London Proceedings Series A*, 423:301–330, 1989.

[12] P.J. James. Particle deformation during cold isostatic pressing of metal powders. *Powder Metallurgy*, 20:199204, 1977.

[13] J.F. Jeirer, D. Imbault, F.V Donzé, and P. Doremus. A geometric algorithm based on tetrahedral meshes to generate a dense polydisperse sphere packing. *Granular Matter*, 11:43–52, 2009.

[14] J. Kozicki and F.-V. Donzé. A new open-source software developed for numerical simulations using discrete modelling methods. *Computer Methods in Applied Mechanics and Engineering*, 197:4429–4443, 2008.

[15] H. Kruggel-Emden, E. Simsek, S. Rickelt, S. Wirtz, and V. Scherer. Review and extension of normal force models for the discrete element method. *Powder Technology*, 171(3):157 – 173, 2007.

[16] C.L. Martin. Elasticity fracture and yielding of cold compacted metal powders. *Journal of the Mechanics and Physics of Solids*, 52:1691–1717, 2004.

[17] A.T. Procopio and A. Zavaliangos. Simulation of multi-axial compaction of granular media from loose to high relative densities. *Journal of the Mechanics and Physics of Solids*, 53:1523–1551, 2005.

[18] D. Sinisa, S.D. Mesarovic, and N.A. Fleck. Spherical indentation of elastic-plastic solids. In The Royal Society, editor, *Physical and Engineering Sciences*, pages 2707–2728, 8 July 1999.

[19] B. Storkers, S. Biwa, and P.-L. Larsson. Similarity analysis of inelastic contact. *International Journal of Solids and Structures*, 34:3061–3083, 1997.

[20] C. Thornton and S.J. Antony. Quasi-static deformation of particulate media. *Philosophical transactions Royal Society Mathematical, physical and engineering sciences*, 356:2763–2782, 1998.

[21] D.V. Tran, R.W. Lewis, D.T. Gethin, and A.K. Ariffin. Numerical modeling of powder compaction processes displacement based finite element method. *Powder metallurgy*, 36(4):257–266, 1993.

[22] C.Y Wu, A.C.F. COCKS, and O.T GILLIA. Die filling and power transfer. *International journal of powder metallurgy*, 39(4):51–64, 2003.